

Detection of runaway electrons using Cherenkov-type detectors in the ISTTOK Tokamak

V. V. Plyusnin¹, L. Jakubowski², J. Zebrowski², H. Fernandes¹, C. Silva¹, P. Duarte¹,
K. Malinowski², M. Rabinski², M.J. Sadowski².

¹ Association Euratom/IST, Instituto de Plasmas e Fusão Nuclear, Instituto Superior Técnico, Av. Rovisco Pais, 1049 – 001 Lisboa Portugal

² Association Euratom/IPPLM, The Andrzej Soltan Institute for Nuclear Studies (IPJ), 05-400 Otwock-Swierk, Poland

1. Introduction. In low-density plasmas at high toroidal electric fields, like in the ISTTOK tokamak, the runaway electron generation is inevitable. Such plasmas are usually unstable due to obvious non-Maxwellian properties of the electron distribution function deteriorating the reliability of measurements. The low energy threshold for runaway regimes and fast escape of electrons without gaining detectable energy make difficult the characterization of runaways and assessment of their influence on plasma performance. In the past the runaway generation regimes in the ISTTOK tokamak have been quantified in a frame of conventional theory of runaway generation using the interpretative modelling of the plasma power-energy balance and calculation of runaway electron current [1-3]. Numerical analysis of the experimental data provided an adequate discharge description and characterization of the runaway generation process in ISTTOK. The evaluated density of runaway electrons was around 0.1-1% of the background plasma density providing up to 30% of the total plasma current [1-3].

This paper presents the recent experiments aiming at the direct observation of the runaway electrons using the Cherenkov-type detector. This detector has been specially designed for the measurements of energetic electrons in tokamak plasma [4-6]. Using this detector the population of electrons with energies higher than the runaway energy threshold in low current (3-4 kA) discharges has been observed. A comparison of the results of numerical simulation to the experimental data yields close their correspondence in energies values and in spatial and temporal characteristics.

2. Cherenkov-type detectors used on the ISTTOK tokamak. A charged particle moving through a transparent medium with a velocity higher than the phase velocity of light in this medium emits radiation, which is called Cherenkov radiation. Such radiation is emitted nearly immediately (with a delay of about 0.1 ns), and its intensity is very high. Emitted energy increases with an increase in particle energy (velocity), and it is larger for a medium with a large refraction coefficient. The properties of several materials have been studied to determine the most appropriate one to be used as a radiator of the Cherenkov emission [4-6]. Parameters of these materials are presented in Table 1.

Material	Refraction index	Lower electron energy threshold [keV]	Thermal conductivity [W/cm K]
Glass	1.8	104	0.01
Aluminium nitride	2.15	66	1.7
Diamond	2.42	51	20
Rutile (TiO ₂)	2.9	33	0.12

Table 1.

Analysis of the values of refraction index and corresponding minimal energy threshold of the detected particles for different materials shows that aluminium nitride (AlN) is one of the

most appropriate materials to be used as a radiator of the Cherenkov emission in plasma experiments. This material has an energy threshold about 66 keV, and it has not been damaged by the exposure to ISTTOK plasmas. A detector of the Cherenkov emission was manufactured at the IPJ (Poland). It consists of a detecting head, a thin-wall metal tube and a fibre optical cable (Figure 1).

The measuring detector head consists of an AlN crystal protected by a 10- μm titanium layer. The detector has a circular input window (collimator) of 5 mm in diameter. The collimator, which was oriented at the angle of 45° in relation to the vacuum chamber axis, together with radiator coating has enabled the detection of fast electrons with the energies above 80 keV. The Cherenkov emission signal has been transmitted from the radiator along a thin-wall metal tube (with the well-polished inner surface) to a connector of the fibre cable at the second end of the tube. This construction has enabled the elimination of detrimental scintillations in the first part of the light-carrying channel. The Cherenkov radiation is then transmitted through an optical cable to a fast photomultiplier with a sampling frequency 2 MHz. All parts of the detector were mounted on a movable support, which was inserted into the vacuum chamber through the horizontal diagnostic port. The construction enabled the measurements from a position where the detector is well hidden inside the diagnostic port ($r > 10$ cm), until $r_{probe} \approx 55$ mm, where detector starts to disturb the discharge.

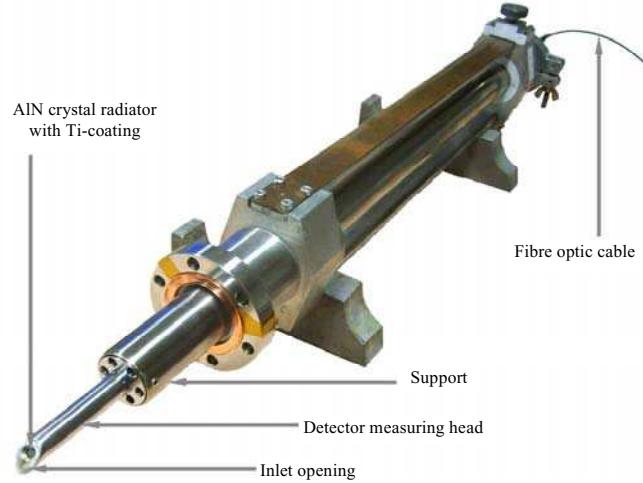


Figure 1. View of the detector used for the measurements of Cherenkov emission in ISTTOK.

3. Detection of runaway electrons on different stages of the ISTTOK discharges. Figure 2 presents typical time traces of the main plasma parameters in ISTTOK: plasma current I_{pl} , average density $\langle n_e \rangle$, loop voltage V_{loop} and electron temperature $T_e(t)$, evaluated using two approaches: inferred from the plasma resistance on the basis of the Spitzer's resistivity; and by the 0-D power-energy balance modelling [1-3] using the measured macroscopic plasma parameters. The data on evolution of the electron temperature is necessary for the modelling of runaway process. In the first case the conventional formula has

been used: $T_e^{Sp}(t) = [C_g * Z_{eff} * f(Z_{eff}) \ln \Lambda * I_{pl}(t) / V_{loop}(t)]^{2/3}$, where C_g is a numeric coefficient, which includes the dependence on the geometrical parameters of the device, and $f(Z_{eff})$ is the resistivity correction factor in impure plasmas. Spectroscopic measurements indicated the presence of the impurities, but it was not possible to evaluate accurately the values of Z_{eff} . That is why a self-consistent 0-D transport modelling has been used for the determination of

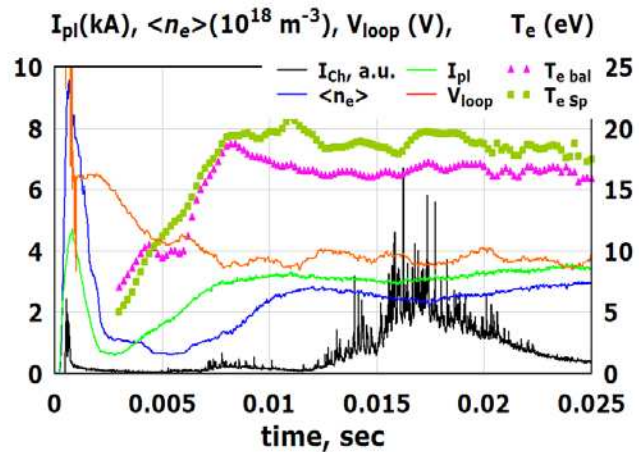


Figure 2. Typical evolution of the main plasma parameters including the evolution of calculated electron temperature and the signal from the detector of Cherenkov radiation.

$T_e(t)$. In this modelling the measured global plasma parameters were used as ‘stiff’ boundary conditions. Average $T_e(t)$, $n_{RA}(t)$ and $I_{RA}(t)$ were calculated by iterations using values of Z_{eff} as an iterative parameter to achieve the minimal deviations between the experimental $I_{pl}(t)$ and $V_{loop}(t)$ values and those provided by the simulations taking into account calculated values of $T_e(t)$ and $I_{RA}(t)$.

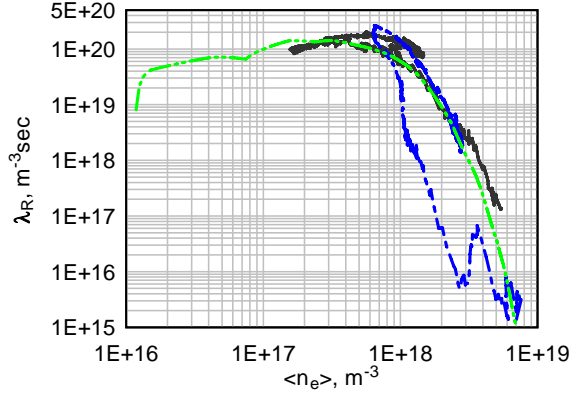


Figure 3. Trends in runaway electron generation: λ_R calculated vs. plasma density for several shots in ISTTOK

The initial values of the electric field $E_0 = V_{loop}/2\pi R_0 \approx 8-10$ V/m provided the break-down of the working gas and creation of the plasma with a line-averaged density ranging up to $\langle n_e \rangle = (7-10) \cdot 10^{18} \text{ m}^{-3}$, which corresponds to a fairly complete ionization of neutral hydrogen in a vacuum chamber at $p_0 = (1-1.5) \cdot 10^{-4}$ torr. The observed burst of the Cherenkov emission at the beginning of the discharge signifies that high E_0 applied for discharge initiation and pressure of the neutral gas in the vacuum chamber have provided the conditions for runaway electron generation at the beginning of the ISTTOK discharges. The Cherenkov emission signals disappear or decrease significantly after increase of the average plasma density up to $\langle n_e \rangle \approx (7-10) \cdot 10^{18} \text{ m}^{-3}$ during the first 0.5-2 ms of the discharge resulting in the almost complete suppression of the runaway generation. As typically observed in small devices, the runaway regimes in ISTTOK are caused by the classical Dreicer mechanism, which is characterized by runaway production rate: $\lambda_R \approx C(Z_{eff}) \varepsilon^{-3(Z+1)/16} n_e v_e \exp\{-1/4\varepsilon - ((Z+1)/\varepsilon)^{1/2}\}$, where e is the electron charge, $v_e = 2.91 \cdot 10^{-6} \ln \Lambda n_e Z_{eff} T_e^{-3/2}$ is the electron collision frequency, $\varepsilon = E_0/E_{DR}$, $E_{DR} = e^3 \ln \Lambda n_e Z_{eff} / 4\pi \varepsilon_0^2 T_e$ is the Dreicer critical field, Z_{eff} is the effective ion charge and $\ln \Lambda$ is the Coulomb logarithm. Evaluation of the data at the beginning of the ISTTOK discharges shows that as the plasma density increases up to $(7-10) \cdot 10^{18} \text{ m}^{-3}$ the runaway production rate could decrease more than 5 orders of magnitude (Figure 3). However, a further evolution of the majority of discharges is characterised by the high probability of the runaway generation due to a significant decrease of the plasma density and obvious increase of the runaway generation rate (Figures 2 and 3). Simultaneously to or with a small time delay after density drop the signal of the Cherenkov emission increases again demonstrating the appearance of fast electrons. In some shots the Cherenkov signal lasts during the whole 20-30 ms of the pulse length. A confirmation that the signal from the probe was caused by the presence of unidirectional flux of the fast electrons in the investigated ISTTOK plasmas has been obtained in experiments with alternate current discharges. The appearance of the Cherenkov signal from the detector was observed only when the probe collimator had the orientation along the direction of the plasma current, i.e. when the electron flux (penetrating through the collimator) could interact with the detector crystal.

The runaway process, studied experimentally using Cherenkov-type detector, has been analysed in a frame of a test particle model [7]. This modelling allowed an assessment

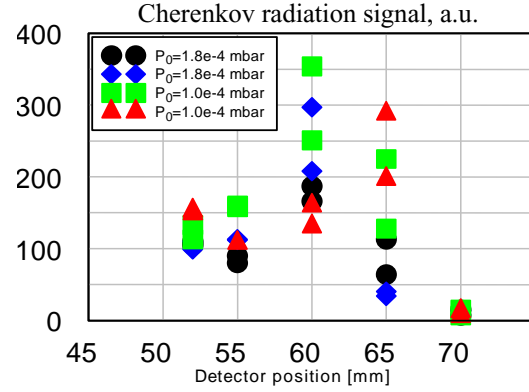


Figure 4. Spatial characteristics of the Cherenkov radiation obtained in the different series of the ISTTOK discharges.

of the kinetic energy ranges of runaway electrons expected in the ISTTOK discharges. The numerical simulation and evaluation of the kinetic energy values of the electrons in several discharges with observed runaway generation has yielded $1.08 \leq \gamma \leq 2.3$. These results adequately correspond to the detector measuring capabilities (energy threshold equal to about 80 keV, that corresponds to $1.15 \leq \gamma \leq 1.2$), confirming earlier results of runaway electron studies carried out on the ISTTOK tokamak. Calculation of the runaway electron density yielded the values, at which the runaway electron current could achieve up to 1 kA.

Figure 4 presents a short summary on the spatial characteristics of the Cherenkov radiation obtained at different initial experimental conditions and shown as a function of neutral gas pressure. This data is in adequate agreement with the issues of the conventional theory of the runaway electrons [8,9]. It is known that the runaway electron orbit outward drift increases with an increase of the runaway energy according to the following expression: $\gamma = (1 + [(1 - \rho_{RA}/a_{pl}) * 2R_0/a_{pl} * I_{pl}/I_A]^2)^{1/2}$, where ρ_{RA} - the initial runaway orbit radius and I_A - Alfvén current. Under given condition ($I_{pl} = 3$ kA) one can obtain that maximal accessible electron energy is $\gamma_{max} \leq 2.2$ in the case it is generated at $\rho_{RA} = 0$. From other hand the detecting energy threshold resulted in cut-off for electrons with lower energies. Therefore, Cherenkov probe is capable to detect the runaway electrons born not only at the probe position but the ones generated inside the radius of the performed measurements.

4. Summary. A new detector for the measurements of Cherenkov radiation emitted at the interaction of energetic electrons (super-thermal and runaways) with AlN crystal was designed, manufactured and installed on the ISTTOK tokamak. Using this Cherenkov-type detector the runaway generation regimes have been identified in the low-current ISTTOK discharges confirming previous results obtained by the numerical analysis of macroscopic plasma parameters. The population of the runaway electrons with energy higher than 80 keV has been recorded. Their energy is obviously higher than the critical energy for runaway the process in ISTTOK. The numerical evaluation of the experimental data has revealed that such electrons can be generated at the vicinity of the plasma centre and they can be detected at the probe position.

5. Acknowledgement. This work has been carried out in the frame of the Contract of Association between the European Atomic Energy Community and Instituto Superior Tecnico. It also received financial support from Fundacao para a Ciencia e a Tecnologia (FCT), Portugal. This research has been also partially supported by the European Communities under the contract with the Association EURATOM-IPPLM, Poland (task P3), and by the Ministry of Science and Higher Education (Poland) under the contract No. 504-1/EURATOM/2008/7'. The content of the publication is the sole responsibility of the authors and it does not necessarily represent the views of the Commission of the European Union or FCT or their services.

References

- [1] V.V. Plyusnin et al. Plasma Phys. Contr. Fusion 44 (2002) 2021–2031
- [2] V.V. Plyusnin et al. Review of Scientific Instruments 74(March 2003) 1807-1810
- [3] V.V. Plyusnin et al. Journal of Nuclear Materials 313-316 (2003) 1052-1055.
- [4] M.J. Sadowski, L. Jakubowski, A. Szydłowski. Czech. J. Phys. 54 Suppl. C (2004) C74
- [5] L. Jakubowski et al. 34th EPS Conf. on Plasma Physics, Vol.31F (2007) P-5.097
- [6] L. Jakubowski, M. Sadowski, J. Zebrowski, J. Techn. Phys. 38 (1997) 141
- [7] V.V. Plyusnin et al. Nuclear Fusion 46(2006) 277
- [8] V.V. Parail, O.P. Pogutse in: Review of Plasma Physics, Vol. 11, ed. by M.A. Leontovich, Consultants Bureau, New York, 1986.
- [9] H. Knoepfel, D.A. Spong, Nuclear Fusion, 19 (1979) 785